Phase Transitions in $[Fe_3O(OOCCD_3)_6(C_5H_5N)_3](C_5H_5N)$: Evidence from Incoherent Neutron Scattering

Roderick D. Cannon,[†] Upali A. Jayasooriya,*[,†] Samuel K. arapKoske,[†] Ross P. White,[‡] and Jeffrey H. Williams*[,‡]

Contribution from the School of Chemical Sciences, University of East Anglia, Norwich NR4 7TJ, England, and the Institut Laue-Langevin, Grenoble, France.
Received August 27, 1990

Abstract: For $[Fe_3O(OOCCD_3)_6(C_5H_5N)_3](C_5H_5N)$ elastic and quasielastic incoherent neutron scattering measurements are shown to give information on structural reorganization and molecular motions which correlates well with data derived from heat capacity measurements. Phase changes are identified, and clear evidence is obtained for a large increase in molecular motion between 200 and 300 K.

$[Fe_3O(OOCCD_3)_6(C_5H_5N)_3](C_5H_5N)$ contains a mixed-valence cluster of composition $2Fe^{3+} + Fe^{2+}$. X-ray crystallography[1] and solution NMR spectroscopy[2] at room temperature disclose no differences between the Fe atoms, but infrared spectroscopy[3] clearly indicates that the two oxidation states are distinct on the time scale of molecular vibrations. The oxidation states are evidently averaged by a thermal electron hopping mechanism at a rate intermediate between the infrared and NMR time scales. This is supported by Mössbauer and other data of Hendrickson, Sorai, and co-workers.[4]

In the crystal, between each pair of trinuclear cluster molecules there is a nonbonded pyridine molecule, the plane of which contains the crystallographic 3-fold axis (see Figure 1). Specific heat data of Sorai et al.[4b] indicate sharp phase transitions at 111.4 and 112.0 K (T_{c4} and T_{c3}) and at 185.8 K (T_{c2}) another sharp transition overlapped by a gradual one which sets in about 111 K and culminates in a maximum of C_p at 191.5 K (T_{c1}). Figure 2a shows the variation of entropy with temperature as calculated by Sorai et al. T_{c2} is associated with the onset of rotation of the extra pyridine molecules about the C_3 axes, and possibly it corresponds with the temperature at which thermal electron transfer becomes rapid compared with the Mössbauer spectroscopic time scale.[5]

In the course of our studies of electron transfer, we have begun using neutron scattering to probe the dynamics of molecular motion in mixed valence compounds. We report here observations of the temperature dependence of the elastic and quasielastic incoherent scattering from this iron(III,III,II) mixed-valence material, which correlate strikingly with the above phase changes.

Experimental Section

Materials. The aquo-adduct $[Fe_3O(OOCCD_3)_6(H_2O)_3]\cdot 2H_2O$ was prepared by a modification of the method of Chrētien and Lous.[7] To a solution of sodium hydroxide (7.0 g, 0.175 mol) and perdeuterioacetic acid (72.5 mL, 1.1 mol) in water (210 mL) in a large Petri dish was added with stirring powdered iron(II) chloride, $FeCl_2\cdot 4H_2O$ (15.0 g, 0.075 mol). The clear pale green or pale orange solution was left to stand for up to 2 weeks, open to air but protected from dust. The product, shiny black crystals, was filtered off under nitrogen, washed once with deoxygenated dilute deuterioacetic acid, and dried for a short time under a stream of nitrogen previously passed through P_2O_5. Yield: typically 7.0 g. Standard C and H microanalyses were carried out on CH_3-containing samples prepared in the same way. Iron(II) was determined by dissolving weighed portions in deoxygenated dilute aqueous sulfuric acid and titrating potentiometrically with cerium(IV). The total iron content was determined by the same method after reducing all iron(III) to iron(II) with amalgamated zinc. Calcd: C, 23.63; H, 4.30; Fe(II), 9.16; Fe(total), 27.47. Found: C, 23.63; H, 4.03; Fe(II), 8.48; Fe(total), 25.70. Although the ratio Fe(II)/Fe(total) was often slightly low in these preparations, the ratios in the pyridine adducts prepared from them were satisfactory as noted below.

The aquo-adduct (7.2 g, ca. 0.012 mol) was placed in a dry 3-necked round-bottomed flask fitted with tap funnel and Schlenk-type filter tube. After deoxygenation by passing dry nitrogen, deoxygenated deuteriopyridine (38 mL, 0.47 mol) was quickly added, and the mixture was vigorously stirred. The solid dissolved rapidly with slight evolution of heat, and after the mixture was stirred for 30 min to 1.5 h the pyridine complex was filtered off under nitrogen. The product was stored slightly damp with pyridine and allowed to dry in a helium atmosphere just prior to the measurements. Typical yields were 75% based on the aquo-adduct. Samples prepared in this way consistently gave satisfactory infrared spectra[3] and analyses. Iron(II) and total iron were determined as above. Calcd: Fe(II), 6.26; Fe(total), 18.78. Found: Fe(II), 6.25; Fe(total), 18.66. Pyridine was determined by treating weighed portions with excess dilute aqueous sodium hydroxide and steam-distilling in a specially constructed one-piece glass apparatus.[8] The vapors were condensed into excess dilute aqueous hydrochloric acid, and this was back-titrated with alkali, potentiometrically, with use of a glass electrode. Two end-points were observed, corresponding to the consumption of excess H^+ and $[pyH^+]$, respectively. Found: 4.02 mol of pyridine per mol of $[Fe_3]$. Excessive drying with nitrogen led to samples with low pyridine content.

Measurements. Incoherent quasielastic neutron scattering measurements were carried out at the Institut Laue-Langevin with use of the back-scattering spectrometer IN13 and the time-of-flight spectrometer IN5. In both cases the samples were placed in aluminum containers and temperatures were controlled with a liquid helium cryostat. Measurements were also taken on the empty containers and on vanadium standards, to estimate background effects and detector efficiencies. Data treatment and manipulation were carried out with in-house programs.

Results and Discussion

We first give the results from a fixed energy-window scan.[9] In this type of experiment, neutrons scattered elastically from the sample are detected over a range of angles, so that the analysis corresponds to a determination of the spectral intensity at $\omega \approx 0$. It is the instrument resolution which defines the actual energy range over which the analysis is performed, and in the present work on IN13 this corresponds to ca. 8 μeV. Scattering is dominated by the ^1H atoms, which in our sample are only present in the pyridine ligand and solvate molecules. The methyl groups,

[†] University of East Anglia.
[‡] Institut Laue-Langevin.

(1) Woehler, S. E.; Wittebort, R. J.; Oh, S. M.; Kambara, T.; Hendrickson, D. N.; Inniss, D.; Strouse, C. E. *J. Am. Chem. Soc.* **1987**, *109*, 1063.
(2) White, R. P.; Wilson, L. M.; Williamson, D. J.; Moore, G. R.; Jayasooriya, U. A.; Cannon, R. D. *Spectrochim. Acta* **1990**, *46A*, 917.
(3) (a) Cannon, R. D.; Montri, L.; Brown, D. B.; Marshall, K. M.; Elliott, C. E. *J. Am. Chem. Soc.* **1984**, *106*, 2591. (b) Meesuk, L.; Jayasooriya, U. A.; Cannon, R. D. *J. Am. Chem. Soc.* **1987**, *109*, 2009.
(4) (a) Oh, S. M.; Kambara, T.; Hendrickson, D. N.; Sorai, M.; Kaji, K.; Woehler, S. E.; Wittebort, R. J. *J. Am. Chem. Soc.* **1985**, *107*, 8009. (b) Sorai, M.; Kaji, K.; Hendrickson D. N.; Oh, S. M. *J. Am. Chem. Soc.* **1986**, *108*, 702.
(5) (a) Kambara, T.; Hendrickson, D. N.; Sorai, M.; Oh, S. M. *J. Chem. Phys.* **1986**, *85*, 2895. (b) Stratt, R. M.; Adachi, S. H. *J. Chem. Phys.* **1987**, *86*, 7156.
(6) Lupu, D.; Ripan, R. *Rev. Roum. Chem.* **1971**, *16*, 43.
(7) Chrētien, A.; Lous, E. *Bull. Soc. Chim. Fr.* **1944**, *11*, 446.
(8) The design was provided by Professor G. Davies, Chemistry Department, Boston University, Boston, MA 02115.
(9) Springer, T. In *Dynamics of Solids and Liquids by Neutron Scattering*; Lovesey, S. W., Springer, T., Eds.; Springer-Verlag: Berlin, 1977; Chapter 5, p 284.

0002-7863/91/1513-4158$02.50/0

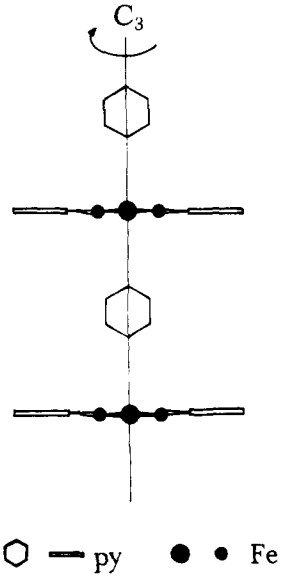

Figure 1. Structural units in the crystal of $[Fe_3O(OOCMe)_6(C_5H_5N)_3](C_5H_5N)$ (adapted from ref 1).

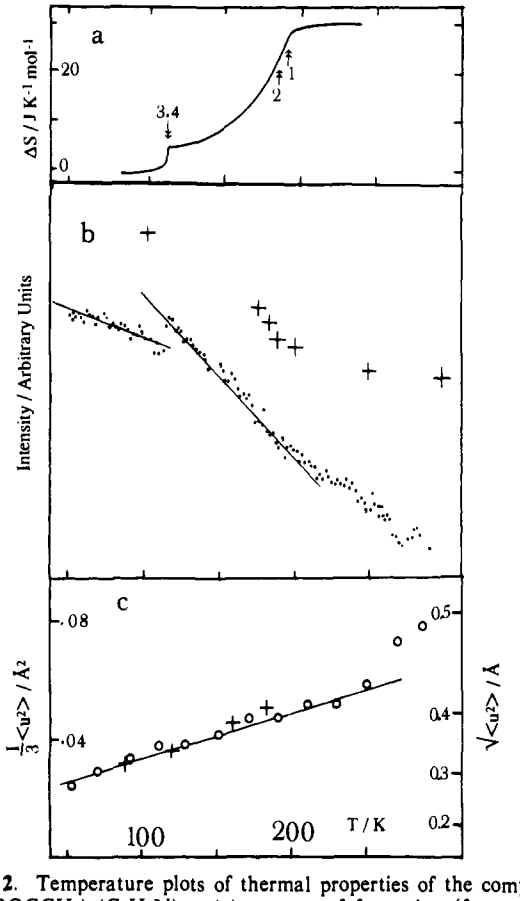

Figure 2. Temperature plots of thermal properties of the compound $Fe_3O(OOCCH_3)_6(C_5H_5N)_4$: (a) entropy of formation (from ref 4), arrows with numbers indicate the phase transition temperatures T_{c1}, etc.; (b) incoherent neutron scattering intensity [(○) elastic scattering intensity $S(Q\omega \approx 0)$, from scans over the fixed window of $(h/2\pi)\omega = \pm 8$ μeV; (+), quasielastic scattering intensity, $S(Q,\omega)$ integrated over the range $(h/2\pi)\omega = \pm 1$ meV]; (c) values of d ln $[S(Q,0)]/d(Q^2)$ [(○) derived from the plots in Figure 3a; (+) from Figure 3b].

which are known to rotate about the C–C bonds of the acetate ions at temperatures even as low as 100 K, are fully deuterated and do not contribute significantly to the scattering.

The elastic scattering probability function is defined as $S(Q,\omega)$, where $S(Q,\omega)\,dQ\,d\omega$ is the probability of scattering a neutron with momentum transfer in the range Q to $Q + dQ$ and energy transfer in the range ω to $\omega + d\omega$. For the fixed-window case this is given by[9]

$$S(Q,\omega \approx 0) = c \exp(-Q^2\langle u^2\rangle/3) \qquad (1)$$

where c is proportional to the number of scatterers in the sample and $\langle u^2\rangle$ is the mean square amplitude of motion of the scatterers. Values of $S(Q,\omega \approx 0)$ summed over the momentum range Q = 1.19–1.99 Å^{-1} are plotted against sample temperature in Figure 2b (middle curve).

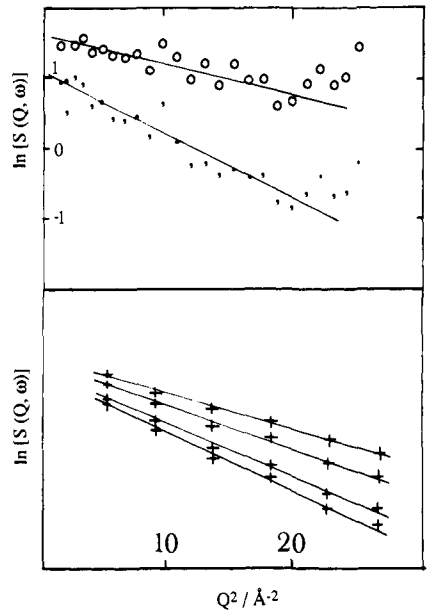

Figure 3. Plots of ln $S(Q,\omega \approx 0)$ against Q^2: (a, top) Data from fixed-window measurements of $S(Q,\omega \approx 0)$ at T = 51 (○) and T = 287 K (•). Straight lines are drawn by least-squares fitting, omitting the points at the three highest Q values. (b, bottom) Data derived from scans of $S(Q,\omega)$ in the quasielastic range, $(h/2\pi)\sum = \pm 4$ μeV, interpolated at ω = 0. Temperatures, reading downwards, T = 90, 120, 160, 184 K.

The curve is evidently in three sections. A low-temperature region below ca. 115 K corresponds to the phase previously characterised by Sorai, Hendrickson, and co-workers as having complete valence localization. The triangular iron clusters are presumed to be ordered in domains, with the local C_2 axes parallel.[1,4,5] Between 110 and 115 K there is a marked discontinuity in the curve. The value of $S(Q,\omega \approx 0)$ increases abruptly and this implies a sudden increase in the number of moving, scattering centers. This discontinuity corresponds well with the previously reported sharp phase transitions T_{c3}, T_{c4}, which have been interpreted as order–disorder transitions. Here it is thought that intermolecular interactions are overcome by thermal fluctuations and there is conversion to a disordered mixture of electronically localized and delocalized (non-distorted, valence-equivalent) Fe_3 clusters.[5] In other words, the ground-state adiabatic potential energy surface changes at these temperatures. On raising the temperature above these transitions, rates of intramolecular electron transfer have been reported to increase rapidly, from ca. 3.1 × 10^4 s^{-1} (NMR) to greater than 10^7 s^{-1} (Mössbauer) at 190 K. This corresponds to the steepest portion of the elastic scattering curve (Figure 2b). Finally, above ca. 190 K, the gradient of the curve becomes less, a change which corresponds either to T_{c2} or to the heat capacity maximum at T_{c1}.

In a further experiment on IN5, quasielastic scattering was measured over a much wider energy range, and from these data, integrated values of $S(Q,\omega)$ over the range −1 to 1 meV were extracted. The plot of these values against temperature, shown as additional points in Figure 2b, also shows a steep fall from ca. 100 to 190 K, and a change of gradient close to T_{c2} and T_{c1}. The loss of elastic scattering intensity over the middle temperature region reflects an increase in inelastic and quasielastic scattering outside the energy windows we have used, i.e. at energy transfers in excess of 1 meV. This implies increasing thermal population

of magnetic, librational, and vibrational levels. Inelastic features have indeed been observed in the range 3–50 meV, and these will be the subject of a future investigation.[10]

Returning to the fixed-window data, plots of ln $[S(Q,\omega \approx 0)]$ versus Q^2 give straight lines from which $\langle u^2 \rangle$ can be calculated (see eq 1). Typical plots are shown in Figure 3a. There is considerable scatter, because (1) each point represents only 4.75 min of data collection at the low neutron flux used and because (2) while corrections for detector efficiency have been applied, contributions from Bragg scattering have not been eliminated. What can be seen however is a clear difference in gradient, implying different amplitudes of proton motion, between the lowest (51 K) and the highest (287 K) temperatures. To confirm this, a second set of experiments was performed, scanning over a range of ω. Data in the range $(h/2\pi)\omega = -4$ to $+4$ μeV were extracted from these scans and taken as measures of $S(Q,0)$. Only four temperatures were used, but the measuring time was extended to 20 h in each case, and the detectors were regrouped, so that sets of four consecutive angles were summed together. With all these improvements in the statistics, plots of ln $[S(Q,0)]$ versus Q^2 gave much better straight lines, as shown in Figure 3b.

Values of $\langle u^2 \rangle^{1/2}$ obtained by these two methods are plotted against temperature in Figure 2c and can be seen to agree well. In the range 50–220 K, values go from 0.28 to 0.4 Å, and there is no break in the curve near 112 K, in contrast to the elastic scan data shown in Figure 2b. The gradient of the curve however increases over the range 230–287 K, with $\langle u^2 \rangle^{1/2}$ reaching about 0.5 Å at the upper end of the range. Contributions to $\langle u^2 \rangle^{1/2}$ come from all moving parts of the molecule, but they are dominated by the hydrogenous parts, i.e. the pyridine molecules. In the crystal structure[5] the coordinated pyridines are stacked parallel to each other, as shown in Figure 1, and their motions must be relatively restricted; hence the increase in $\langle u^2 \rangle^{1/2}$ must reflect mainly motions of the noncoordinated pyridines, which are held only by weak lattice forces. Within the statistics, the data are consistent with the onset of rotational motion at around $T = T_{c1} \approx 190$ K. Quasielastic scattering experiments are in progress to characterize this motion more precisely.

Conclusion

What is clear from the present work is that there are striking correspondences between the elastic scattering probability and other physical measurements, especially the specific heat data of Sorai et al. In particular, the first-order transition shown by the specific heat data coincides with a discontinuous change in the scattering probability, while the second-order transition coincides with a gradual change in the gradient of the scattering profile. The steepest gradient of the profile agrees with the region of maximum entropy gain of the sample.

Acknowledgment. We thank the Science and Engineering Research Council for the provision of beam time and the Kenya State Ministry of Education for a scholarship to S.K.a-K.

(10) Jayasooriya, U. A.; Cannon, R. D.; arapKoske, S. K.; Anson, C. E.; White, R. P.; Kearley, G. D. ILL Experimental Report 9-08-39 (January, 18, 1991); full manuscript in preparation.

Unprecedented and Reversible Cobalt-to-Carbon Alkyl Bond Rearrangement in the Coenzyme B_{12} Model Complex $C_6H_5CH_2Co^{III}[C_2(DO)(DOH)_{pn}]I$: Synthesis, Structural Characterization, and Mechanistic Studies

Brian E. Daikh[1] and Richard G. Finke*

Contribution from the Department of Chemistry, University of Oregon, Eugene, Oregon 97403. *Received October 26, 1990*

Abstract: Photolysis of the coenzyme B_{12} model complex $PhCH_2Co[C_2(DO)(DOH)_{pn}]I$ (**1**) leads to a high-yield, efficient synthesis of an unprecedented cobalt-to-carbon alkyl rearrangement product $Co[C_2(DO)(DOH)_{pn}CH_2Ph]I$ (**2**), (*SP*-5-15)-[2-[[3-[[2-(hydroxyamino)-1-methyl-2-(phenylmethyl)butylidene]amino]propyl]imino]-3-pentanone oximato(2-)-*N*,*N*′,*N*″,*N*‴]iodocobalt. The novel product **2** is unequivocally characterized by X-ray crystallography, ^{1}H NMR, visible, and mass spectroscopy, and an elemental analysis. With pure **2** available, a thermal equilibrium between **1** and **2**, $K_{eq} = 1.5 \pm 0.1$ (69 °C, benzene solvent), is shown to exist, thereby explaining the low (60%) yield of **2** from the thermolysis of **1** at 69 °C. Thermolysis of **2** in the presence of TEMPO free radical trap quantitatively yields trapped benzylTEMPO and $^{\bullet}Co^{II}[C_2(DO)(DOH)_{pn}]I$. An Eyring plot of this reaction yields $\Delta H^{\ddagger} = 26 \pm 2$ kcal/mol, $\Delta S^{\ddagger} = -6 \pm 7$ cal/(mol·K), or $\Delta G^{\ddagger}_{298} = 27 \pm 3$ kcal/mol; the $\Delta H^{\ddagger}$ value plus appropriate corrections imply a low benzyl–carbon bond dissociation energy of 25 kcal/mol in **2**. Also provided are a proposed mechanism for the formation of **2**, a summary discussion detailing the significance of the results toward explaining a number of related, but poorly understood, literature reports, and a short list of some interesting but unanswered questions that form a basis for future research.

Previously,[2] in developing the now widely used[3-5] nitroxide radical trapping method for studying cobalt–carbon[3,4] and other metal–carbon[3,5] bond homolyses, we examined the thermolysis of the orange-brown benzyl coenzyme B_{12} model complex

(1) (a) Undergraduate research associate and University of Oregon Honors College Thesis Student. (b) Daikh, B. E., Synthesis Characterization, and Kinetic and Mechanistic Studies of an Unusual Cobalt-to-Carbon Bond Alkyl Rearrangement in the Coenzyme B_{12} Model Complex $C_6H_5CH_2Co^{(III)}[(DO)(DOH)_{pn}]I$. University of Oregon Honors College Thesis, Eugene, OR, May 9, 1990.

(2) (a) Finke, R. G.; Smith, B. L.; Mayer, B. J.; Molinero, A. A. *Inorg. Chem.* **1983**, *22*, 3677. (b) Smith, B. L. Ph.D. Dissertation, University of Oregon, Eugene, OR, 1982. (c) Aromatic solvents were used[2a,b] since formation of $PhCH_3$ by H$^{\bullet}$ abstraction from the solvent cannot[2a,b] occur given thermochemical ($PhCH_2$–H versus Ph–H bond energy) considerations.

0002-7863/91/1513-4160$02.50/0